

Giant van der Waals and Casimir interactions via transmission lines

Ephraim Shahmoon,¹ Igor Mazets,^{2,3} and Gershon Kurizki¹

¹*Department of Chemical Physics, Weizmann Institute of Science, Rehovot, 76100, Israel*

²*Vienna Center for Quantum Science and Technology, Atominstitut, TU Wien, 1020 Vienna, Austria*

³*Ioffe Physico-Technical Institute of the Russian Academy of Sciences, 194021 St. Petersburg, Russia*

(Dated: April 9, 2013)

We show that the van der Waals (vdW) and Casimir forces between neutral particles can be enhanced by many orders of magnitude upon changing the character of the force-mediating vacuum photon-modes. By considering two induced dipoles in the vicinity of any standard electric transmission line, where photons can propagate in one dimension (1d), we find analytically that the interaction scales nontrivially with the inter-dipolar distance, resulting in much stronger and longer-range interaction than in free-space. This may have profound implications on the non-additivity of vdW and Casimir interactions in many-particle systems, and open the door for Casimir phenomena in 1d. We discuss the possibilities of measuring this effect, e.g. in a coplanar waveguide line.

PACS numbers: 03.70.+k, 12.20.-m, 42.50.-p, 31.30.J.-

Introduction. Quantum electromagnetic fluctuations induce forces between neutral particles. This was first shown by London [1], to be a source of the van der Waals (vdW) interaction between two induced dipoles. Casimir and Polder [2] addressed the same interaction as being mediated by virtual photons from the vacuum. For inter-particle distances r shorter than their dipolar-transition wavelength λ (the vdW limit), they found that the interaction energy falls off as $1/r^6$, whereas for longer distances (the retarded, Casimir limit), it scales as $1/r^7$. Vacuum-mediated interactions that scale differently from the $1/r^6$ and $1/r^7$ power laws are known to exist between two polarizable bulk objects rather than point-like dipoles. Casimir considered the interaction between two parallel metal plates due to the vacuum (zero-point) energy and found an attractive force that scales as $1/d^4$, with d being the distance between the plates [3]. Since then, many related effects have been studied, mainly the interactions between dielectric or metallic objects of various geometries [4, 5]. Such experimental [6–9] and theoretical [10–14] studies demonstrate the role of non-additivity and retardation of these dipolar interactions.

A key point in determining how these effects depend on distance is the space dependence of the propagation and scattering of the virtual photon modes that mediate the interaction. In turn, these modes depend on the geometrical shape of the interacting objects. Here, we take a somewhat different approach towards the geometry dependence of vdW and Casimir-related phenomena. Instead of considering the interaction energy of extended objects with different geometries, we revisit the original Casimir-Polder configuration of a pair of point-like dipoles while changing the geometry of their surrounding environment. More specifically, we consider the energy of the interaction between two point-like dipoles, mediated by vacuum photon modes along 1d. The resulting attractive interaction is found to be much stronger and longer-range than its free-space counterpart, where it surpris-

ingly scales as $\text{const.} + (r/\lambda) \ln(r/\lambda)$ and as $1/r^3$ for short and long distances compared to λ , respectively. This enhancement implies a drastic modification of Casimir-related effects for many-body and bulk systems in such a 1d geometry.

The ability to change the geometry of photon vacuum modes, is widely used in quantum optics, e.g. for the enhancement of spontaneous emission [15, 16] and resonant dipole-dipole interactions [17]. Here we consider 1d photon modes in structures that support the propagation of transverse-electromagnetic (TEM) modes, namely modes where the propagation axis, the electric and the magnetic fields, are perpendicular to each other. These are typically the fundamental transverse modes of electric transmission lines (TLs), i.e. waveguides comprised of two conductors as shown in Fig. 1. They possess a dispersion relation $\omega_k = |k|c$ and an electric field-mode function [18]

$$\mathbf{u}_{kj}(\mathbf{r}) = \frac{1}{\sqrt{A(x,y)L}} e^{ikz} \mathbf{e}_j, \quad (1)$$

where z is the propagation axis, L its corresponding quantization length, $A(x,y)$ the effective area in the transverse xy plane, $\mathbf{e}_{j=x,y}$ the polarization unit vector, k and ω_k the wavenumber in the z direction and the angular frequency, respectively, and $c = 1/\sqrt{\mu\epsilon}$ the phase velocity, μ and ϵ being the effective permeability and permittivity of the TEM mode, set by its geometry and materials. Unlike modes of other waveguides, such as optical fibers or hollow metallic waveguides, here the effective area $A(x,y)$ is independent of frequency. Hence, considering its dispersion relation, the TEM mode forms an effective plane wave in 1d. TLs support also higher-order transverse modes, such as the transverse electric (TE) and transverse magnetic (TM) modes in a coaxial TL [18]. However, as was recently shown for metallic waveguides [19], they do not contribute to the long-range interaction, as explained below. The existence of TEM

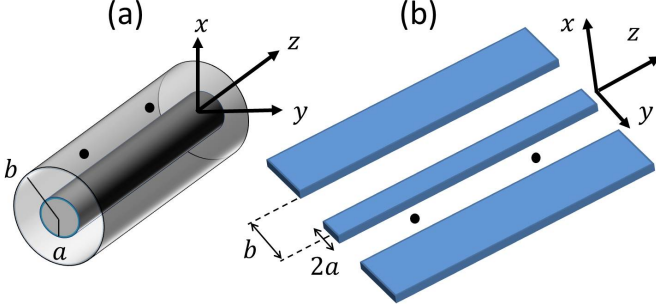


FIG. 1: Geometries of transmission-line mediated vdW and Casimir interactions. (a) Coaxial line: two concentric metallic cylinders, the inner one with radius a and the outer (hollow) one with radius b . Two dipoles represented by black dots are placed in between the cylinders along the wave propagation direction z . They interact via modes of the coaxial line that are in vacuum, giving rise to a vdW-like interaction energy. (b) Coplanar waveguide: similar to (a). Here the central conductor of width $2a$ is separated from a pair of ground plane conductors $2b$ apart.

modes as in Eq. (1) is correct exactly for TLs made from perfect conductors, however it makes an excellent approximation of the propagation of fields in low-loss TLs that are in practical use [18].

Analysis principles. The calculation of the interaction energy contributed by the TEM mode is essentially equivalent to that mediated by the vacuum in 1d. We calculate it analytically by two different methods. In the first, we adopt the quantum electrodynamics (QED) perturbative approach [20]. We consider two identical atomic or molecular dipoles, with a ladder of excited levels $\{|n\rangle\}$, both in their ground state $|g\rangle$, coupled to the vacuum of photon modes given by Eq. (1), via the interaction Hamiltonian

$$H_I = -\hbar \sum_{\nu=1}^2 \sum_{n_\nu} \sum_{k,j} (|n_\nu\rangle\langle g| + \text{h.c.}) (ig_{k,j,\nu} \hat{a}_{kj} + \text{h.c.}) . \quad (2)$$

Here $g_{k,j,\nu} = \sqrt{\omega_k} \mathbf{d}_{n_\nu} \cdot \mathbf{u}_{kj}(\mathbf{r}_\nu)$ is the dipolar coupling between the dipole $\nu = 1, 2$ and the kj field mode, for the $|g\rangle$ to $|n_\nu\rangle$ transition with dipole matrix element \mathbf{d}_{n_ν} , \hat{a}_{kj} being the lowering operator for the kj mode. The vdW energy is then obtained by perturbation theory as the fourth-order correction to the energy of the ground state $|G\rangle = |g_1, g_2, 0\rangle$, where $|0\rangle$ is the vacuum of the photon modes [20],

$$U = - \sum_{I_1, I_2, I_3} \frac{\langle G | H_I | I_3 \rangle \langle I_3 | H_I | I_2 \rangle \langle I_2 | H_I | I_1 \rangle \langle I_1 | H_I | G \rangle}{(E_{I_1} - E_G)(E_{I_2} - E_G)(E_{I_3} - E_G)} . \quad (3)$$

Here $|I_j\rangle$ are intermediate (virtual) states (of the free Hamiltonian) and E_m is the energy of the state $|m\rangle$. The diagram in Fig. 2(a) illustrates one of 12 virtual processes

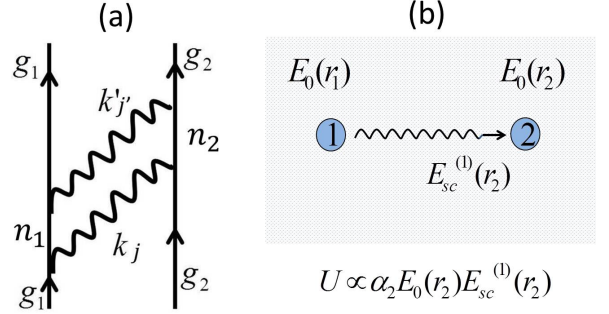


FIG. 2: Calculation methods of interaction energy. (a) QED perturbation theory: one of 12 possible processes (diagrams) that contribute to the energy correction of the state $|G\rangle = |g_1, g_2, 0\rangle$, Eq. (3). Here the intermediate states are $|I_1\rangle = |n_1, g_2, 1_{kj}\rangle$, $|I_2\rangle = |g_1, g_2, 1_{kj} 1_{k'j'}\rangle$ and $|I_3\rangle = |g_1, n_2, 1_{k'j'}\rangle$, where $|1_{kj}\rangle = \hat{a}_{kj}^\dagger |0\rangle$. (b) Scattering of vacuum fluctuations: the vacuum field $\hat{\mathbf{E}}_0(\mathbf{r})$ exists in all space and interacts with both dipoles at their positions \mathbf{r}_1 and \mathbf{r}_2 , hence it is also scattered by the dipoles. The scattered field from one dipole, e.g. 1, $\hat{\mathbf{E}}_{sc}^{(1)}(\mathbf{r})$, arrives at dipole 2, resulting in an interaction interpreted as the vdW/Casimir interaction U .

that contribute to this energy correction (see analysis details below).

A more transparent approach towards this calculation is that of classical electrodynamics in the presence of an external fluctuating (quantum) vacuum field [4]. As shown in Fig. 2(b), we consider two point dipoles with polarizabilities $\alpha_{1,2}(\omega)$, subject to a fluctuating (vacuum) field $\hat{\mathbf{E}}_0$. The electromagnetic energy of, say, dipole 2, is given by a sum over all k of $-(1/2)\alpha_2(\omega_k)[\hat{\mathbf{E}}_k(\mathbf{r}_2)\hat{\mathbf{E}}_k^\dagger(\mathbf{r}_2) + \hat{\mathbf{E}}_{sc,k}^\dagger(\mathbf{r}_2)\hat{\mathbf{E}}_k(\mathbf{r}_2)]$, where $\hat{\mathbf{E}}_k(\mathbf{r}_2)$ is the k mode component of the electromagnetic field at the location of this dipole. The field at \mathbf{r}_2 includes two components: $\hat{\mathbf{E}}_{0,k}(\mathbf{r}_2)$, the external fluctuating (vacuum) field, and $\hat{\mathbf{E}}_{sc,k}^{(1)}(\mathbf{r}_2)$, the scattered field, which to lowest order is that scattered from dipole 1, where it is driven by the external (vacuum) fluctuations $\hat{\mathbf{E}}_{0,k}(\mathbf{r}_1)$ at \mathbf{r}_1 . Since the TEM field exhibits diffraction-less propagation in 1d, this scattered field is found by essentially solving

$$\left(\frac{\partial^2}{\partial z^2} + k^2 \right) \hat{\mathbf{E}}_{sc,k}^{(1)}(z) = -\mu \alpha_1^{(1d)}(\omega_k) \hat{\mathbf{E}}_{0,k}(z_1) \delta(z - z_1), \quad (4)$$

where $\alpha_\nu^{(1d)} = \alpha_\nu/A(x_\nu, y_\nu)$ (see analysis details below). The vdW/Casimir energy is then obtained as the interaction energy between the dipoles, which to lowest order becomes

$$U = -2 \sum_k \alpha_2^{(1d)}(\omega_k) \times \langle 0 | \left[\hat{\mathbf{E}}_{sc,k}^{(1)}(z_2) \hat{\mathbf{E}}_{0,k}^\dagger(z_2) + \hat{\mathbf{E}}_{0,k}(z_2) \hat{\mathbf{E}}_{sc,k}^{(1)\dagger}(z_2) \right] | 0 \rangle . \quad (5)$$

Here we average over the quantized fields with the vacuum state $|0\rangle$, and multiply by 4 to account for both field polarizations j and for the energy at dipole 1 as well. From Eq. (4) it is clear that the scattered field is proportional to $\hat{\mathbf{E}}_{0,k}(z_1)$, such that the vdW/Casimir energy, Eq. (5) depends on the correlation between the vacuum fluctuations at z_1 and z_2 .

Both calculation methods yield the same result for the TEM-mediated interaction energy (see analysis details below). Here, we present the resulting energy for the case where one excited level $|e\rangle$ with energy E_e and corresponding wavelength $\lambda_e = 2\pi\hbar c/E_e$, has a dominant dipole transition, such that all other excited levels $|n \neq e\rangle$ can be neglected,

$$\begin{aligned} U(z) &= -\frac{\pi|\mathbf{d}_e^\perp|^4}{2\epsilon^2 E_e} \frac{1}{A_1 A_2 \lambda_e^2} F(z) \\ F(z) &= \left(4\pi \frac{z}{\lambda_e} + i\right) e^{-i4\pi \frac{z}{\lambda_e}} \text{Ei}(i4\pi \frac{z}{\lambda_e}) \\ &+ \pi \left(1 + i4\pi \frac{z}{\lambda_e}\right) e^{i4\pi \frac{z}{\lambda_e}} + \text{c.c.}, \end{aligned} \quad (6)$$

where $z = |z_2 - z_1|$, is the inter-dipolar distance in the TL propagation direction, $A_\nu = A(x_\nu, y_\nu)$, \mathbf{d}_e^\perp is the projection of the dipole matrix element \mathbf{d}_e on the transverse xy plane, c.c. stands for complex-conjugate and $\text{Ei}(x) = -P \int_{-x}^{\infty} dt e^{-t}/t$ is the exponential integral function. This interaction is attractive and its dependence over the distance z is described by the monotonously decreasing function $F(z)$, plotted in Figs. 3(a) and 3(b). From $F(z)$ we can get the energy dependence at short (vdW regime) and long (retarded, Casimir regime) distances, by expanding it for small and large z/λ_e , respectively,

$$\begin{aligned} F(z \ll \lambda_e) &\approx \pi + 16\pi \frac{z}{\lambda_e} \ln \frac{z}{\lambda_e} + 8\pi[2\gamma - 1 + 2\ln(4\pi)] \frac{z}{\lambda_e} \\ F(z \gg \lambda_e) &\approx \frac{1}{8\pi^3} \frac{\lambda_e^3}{z^3}, \end{aligned} \quad (7)$$

where $\gamma \cong 0.577$ is Euler's constant.

Predictions. The above expressions for the interaction energy in the vdW and Casimir regimes, suggest the possibility of a much stronger interaction than its free-space counterpart. In the nonretarded vdW regime, it decreases very slowly with z compared to the familiar $1/z^6$ scaling, whereas in the retarded Casimir regime, it falls off with a power-law which is four powers weaker than the $1/z^7$ Casimir-Polder interaction.

Let us make this comparison more quantitative by considering a general TL with separation a between its two guiding conductors. It is then reasonable to assume that the effective TEM mode area $A(x, y)$ scales as a^2 , a being the relevant length-scale. For example, in a coaxial line [see Fig. 1(a)], by normalizing the electric field of the TEM mode, we find $\sqrt{A} = \sqrt{2\pi \ln(b/a)}\rho$, with $\rho = \sqrt{x^2 + y^2}$ [18]. Since $a < \rho < b$, taking e.g.

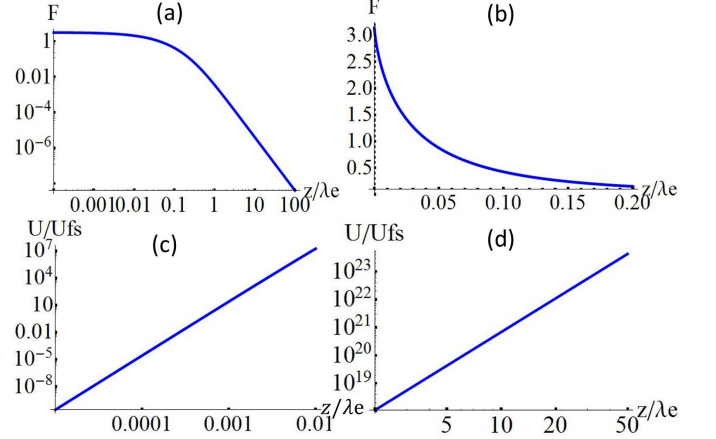


FIG. 3: The TEM-mode mediated interaction potential as a function of inter-dipolar distance z . (a) Log-log plot of $F(z)$, Eq. (6). For long distances, $z \gg \lambda_e$, the linear dependence implies a power-law behavior as in Eq. (7). (b) $F(z)$ at short distances. (c) Log-log plot of the ratio between TEM-mediated energy $U(z)$, Eq. (6), and the free-space vdW energy in short distances $z \ll \lambda_e$, $U_{fs}(z) = -\frac{|\mathbf{d}_e^\perp|^4}{48\pi^2\epsilon^2 E_e} \frac{1}{z^6}$ [20], with $|\mathbf{d}_e^\perp|^2 = (2/3)|\mathbf{d}_e|^2$ and $\sqrt{A_{1,2}} = a$ (see text). Here $a = 10^{-4}\lambda_e$ is taken, consistent with typical cases considered later, where $a \sim \text{few } \mu\text{m}$ and $E_e/(2\pi\hbar) \sim \text{few GHz}$. From $z \sim 10^{-3}\lambda_e$ and beyond, the huge enhancement of the interaction w.r.t its free-space counterpart is apparent. (d) Same as (c), but for long distances $z \gg \lambda_e$ where the free space energy takes the Casimir-Polder form, $U_{fs}(z) = -\frac{23}{64\pi^3} \frac{\hbar c}{\epsilon^2} \frac{4}{9} \frac{|\mathbf{d}_e^\perp|^4}{E_e^2} \frac{1}{z^7}$ [20].

$b = 2a$ and $\rho = a$ we obtain $\sqrt{A} \approx 2.1a$. Moreover, the energy in Eq. (6) depends on the projection of the dipole element on the transverse plane. Assuming the polarizability is isotropic on average, we can estimate $|\mathbf{d}_e^\perp|^2 = (2/3)|\mathbf{d}_e|^2$ (Supplementary Information). Using this estimation with $\sqrt{A_{1,2}} = a$ and taking the reasonable values of $a/\lambda_e < 1$, we calculate the ratio between the TEM-mediated energy and its free-space counterpart. This ratio is plotted in Figs. 3(c) and 3(d) for short and long distances respectively, using the known free-space expressions [20]. From distances as short as $z = 10^{-3}\lambda_e$, the TEM-mediated interaction becomes orders of magnitude stronger, where this ratio increases drastically with z .

At very short distances, however, the free-space vdW interaction $1/z^6$ is stronger. This occurs at $z < a$, where the dipoles are close enough such that they do not "sense" the TL structure. The transition to free-space behavior in this regime can be described by including higher-order transverse modes. These modes become significant at such short distances, where their contributions sum up to give the free-space result. In the Supplementary Information we calculate, for a coaxial TL, the interaction energy due to the TE and TM modes. We find that the

energy contribution of the TE_{lm} and TM_{lm} modes with cutoff frequency ck_{lm} scales like $K_0(k_{lm}z)$ and $e^{-k_{lm}z}$ respectively, where $K_0(x)$ is the modified Bessel function. Since $k_{lm} > \pi/a$, at long distances $z > a$ both decay exponentially and are negligible with respect to the TEM mode energy, however at short distances $z \ll a$, we numerically verify that the dominant TM modes sum up to give exactly the free-space interaction (Supplementary Information). This was also recently shown for the dispersion interaction in a metallic waveguide [19], and we expect it to hold for all TLs. Namely, for distances $z \gg a$ we can indeed consider only the TEM mode, whereas the free-space result is recovered for $z \ll a$, owing to the other transverse modes.

It is important to consider how the predicted effects can be measured. Here we focus on the coplanar waveguide (CPW) TL [21] [Fig 1(b)] that is extensively used in the emerging field of circuit-QED [22–26], and in which the dynamical Casimir effect has been recently demonstrated [27]. We consider the dominant dipole transition of a pair of superconducting transmons [24] at distance z , both capacitively coupled to the CPW. Then, the TEM-mediated interaction should induce a z -dependent energy shift on the dipole-transition levels, $U(z)$ from Eq. (6). In order to estimate this energy shift, we refer to a recent experiment [25], where the dipole frequency is $E_e/(2\pi\hbar) \sim 5\text{GHz}$ and the dipole coupling to a closed CPW cavity of length λ_e , can reach $g \sim \pi \times 720\text{MHz}$. Using $g = \sqrt{\frac{(E_e/\hbar)}{2\epsilon\hbar}} \frac{|\mathbf{d}_e|}{\sqrt{AL}}$ and $L = \lambda_e$ [25, 26], we can extract $|\mathbf{d}_e^\perp|/\sqrt{A}$ for each dipole, obtaining $[U(z)/F(z)]/h \sim 0.84\text{MHz}$, where h is Planck's constant. E.g., for distances $z = 0.001\lambda_e$ or $0.01\lambda_e$ (both much larger than $a \sim \text{few }\mu\text{m}$), the energy shift becomes $U(z)/h \approx 1.8$ or 2.47MHz respectively, about twice the dephasing rate of the dipole, 1MHz [25], that limits the resolution of the shift. However this resolution can be considerably improved, as in Ref. [26], where a dephasing time of about $20\mu\text{s}$ is reported. Then, by taking $E_e/h \sim 2\text{GHz}$ with the parameters of Ref. [25], one can obtain $U(z)/h \approx 28\text{MHz}$ for $z = 0.01\lambda = 1.5\text{mm}$, which is much larger than the dephasing. Probing the interaction in the retarded regime, where $z > \lambda_e$, is currently more challenging: for the latter case, with $z = 2\lambda_e = 30\text{cm}$, we obtain $U(z)/h \approx 6.62\text{KHz}$, which is too small to be observed, although future improvement may make this regime observable as well. Nevertheless, these results imply the remarkable possibility to directly observe the vdW and Casimir interaction between a *single* pair of point-like dipoles (here the size of the dipoles is about $1\mu\text{m}$) over a wide range of macroscopic distances where the interaction scales non-trivially as in Eq. (6).

Moreover, since the open geometry of the CPW allows for the coupling of the TEM mode to clouds of trapped Rydberg atoms or polar molecules above its surface [28, 29], the possibility exists to explore the predicted

long-range interaction in a many-body setting. This may entail a modification of the non-additivity of the vdW and Casimir interactions, which currently attracts considerable interest [5]. In free-space, the vdW energy of a gas is approximately additive, namely it can be obtained by pairwise summation of the vdW energies of all pairs, as long as α/r^3 is small, with r a typical inter-dipolar separation [4]. This scaling is however a direct consequence of dipole-dipole interactions in free space, and is expected to change when the, e.g. atomic dipoles, interact also via the TEM mode of the CPW, for the same reasons that the $1/r^6$ scaling was shown here to change. Such atomic clouds are anticipated to exhibit non-additive effects at smaller densities than usual, which in turn may influence their thermodynamic properties as well as their effective dielectric constant. Furthermore, it will be interesting to consider how the long-range interaction we predict is modified at finite temperatures.

Analysis details. Beginning with the QED perturbative approach, the sum from Eq. (3) includes 12 different terms, each corresponding to a different set of intermediate states and represented by a diagram [20]. E.g. the term corresponding to the diagram from Fig. 2(a) is given by

$$-\frac{\hbar^2 c^2}{16\pi^2 \epsilon^2 A_1 A_2} \sum_{n_1, n_2} (\mathbf{d}_{n_1}^\perp \cdot \mathbf{d}_{n_2}^\perp)^2 \int_{-\infty}^{\infty} dk \int_{-\infty}^{\infty} dk' \times \frac{|k||k'| e^{ikz_{12}} e^{ik'z_{12}}}{(E_{n_1} + \hbar c|k|)(\hbar c|k| + \hbar c|k'|)(E_{n_1} + \hbar c|k'|)}. \quad (8)$$

Summing all 12 terms and then performing the integration over k' we arrive at

$$U \propto \sum_{n_1, n_2} \int_0^{\infty} dk \sin(2kz) \frac{k^2(k + k_{n_1} + k_{n_2})}{(k_{n_1} + k_{n_2})(k + k_{n_1})(k + k_{n_2})}, \quad (9)$$

where $k_n = E_n/(\hbar c)$. Taking a single excited level $|e\rangle$ for each dipole, the integration on k is performed (using regularization) and Eq. (6) is obtained.

Turning to the calculation in the vacuum scattering approach, we observe that the scattered field is proportional to the Green's function of the Helmholtz equation in 1d, Eq. (4), which is found to be $\frac{i}{2|k|} e^{i|k||z-z_1|}$. Then, inserting this field into the energy Eq. (5), where the quantum (vacuum) field in 1d is $\hat{\mathbf{E}}_{0,kj}(z) = i\sqrt{\frac{\hbar\omega_k}{2\epsilon}} \frac{1}{\sqrt{L}} e^{ikz} \mathbf{e}_j \hat{a}_{kj}$ [the index j is suppressed in the Eqs. (4), (5)], we arrive at

$$U = \frac{\hbar c}{2\pi\epsilon^2 A_1 A_2} \int_0^{\infty} dk \alpha_1(k) \alpha_2(k) k^2 \sin(2kz). \quad (10)$$

By assuming the polarizabilities $\alpha_{1,2}$ of a system with a discrete set of transitions as in an atom, $\alpha(k) = \frac{2}{3} \sum_n \frac{E_n |\mathbf{d}_n|^2}{E_n^2 - \hbar^2 c^2 k^2}$ [20], and then transferring the integration to the imaginary axis in a complex k -plane (Wick

rotation, with regularization), we arrive at a result equivalent to that in Eq. (6): it is described by a Meijer G-function, that allows to analytically obtain exactly the same results as in Eq. (7) when $|\mathbf{d}_e^\perp|^2 = (2/3)|\mathbf{d}_e|^2$ is assumed, and can be numerically calculated for a general z .

Conclusions. To conclude, we have studied how transmission-line structures, that are typically used to transmit electromagnetic signals in electronic devices, can in fact transmit vacuum fluctuations between dipoles and drastically enhance dispersion forces. The key point is that the modes of the electromagnetic vacuum are changed in the presence of TLs and include the TEM mode that propagates in 1d. We have shown how the resulting vdW and Casimir-Polder interactions can become longer-range and larger by orders of magnitude than their free-space counterparts. To this end, we have analytically found, via two independent methods, an expression for the dominant TEM-mediated interaction at all inter-dipolar distances, Eq. (6), and described how the free-space result is restored at very short distances, by including higher order modes in our calculations. Our approach assumed that the TL is comprised of perfect conductors at zero temperature. This is justified for a coplanar-waveguide line used in low-temperature, superconducting circuit-QED experiments, for which we have estimated that the effect may be directly measured. We stress that unlike other studies, where the circuit-QED system is used as a single-mode cavity [24, 25, 30], here we consider the open waveguide geometry, which allows for quantum optics in 1d [23].

Our result may pave the way towards further intriguing 1d Casimir effects upon considering extended interacting objects and many-particle systems that are coupled to a transmission line. These configurations may reveal more complex Casimir phenomena than the simple dipole-dipole non-retarded vdW interaction due to two major effects; i.e., retardation and non-additivity [5]. As discussed above, both of these may be drastically modified in a 1d geometry, namely, by the presence of a transmission line.

The support of ISF, DIP, the Wolfgang Pauli Institute and the FWF (Project No. Z118-N16) is acknowledged. We appreciate fruitful discussions with Yoseph Imry and Grzegorz Lach.

[1] F. London, *Trans. Faraday Soc.* **33**, 8-26 (1937).
[2] H. B. G. Casimir and D. Polder, *Phys. Rev.* **73**, 360-372 (1948).
[3] H. B. G. Casimir, *Proc. K. Ned. Akad. Wet.* **51**, 793 (1948).
[4] P. W. Milonni, *The Quantum Vacuum: An Introduction to Quantum Electrodynamics* (Academic, 1993).
[5] A. W. Rodriguez, F. Capasso and S. G. Johnson, *Nature Photon.* **5**, 211 (2011).
[6] A. O. Sushkov, W. J. Kim, D. A. R. Dalvit and S. K. Lamoreaux, *Nature Phys.* **7**, 230 (2011).
[7] D. E. Krause, R. S. Decca, D. Lopez and E. Fischbach, *Phys. Rev. Lett.* **98**, 050403 (2007).
[8] C. C. Chang, A. A. Banishev, G. L. Klimchitskaya, V. M. Mostepanenko and U. Mohideen, *Phys. Rev. Lett.* **107**, 090403 (2011).
[9] J. Munday, F. Capasso, V. A. Parsegian, *Nature* **457**, 170 (2009).
[10] D. A. R. Dalvit, F. C. Lombardo, F. D. Mazzitelli and R. Onofrio, *Phys. Rev. A* **74**, 020101(R) (2006).
[11] T. Emig, R. L. Jaffe, M. Kardar, and A. Scardicchio, *Phys. Rev. Lett.* **96**, 080403 (2006).
[12] R. B. Rodrigues, P. A. Maia Neto, A. Lambrecht and S. Reynaud, *Phys. Rev. Lett.* **96**, 100402 (2006).
[13] M. Levin, A. P. McCauley, A. W. Rodriguez, M. T. H. Reid and S. G. Johnson, *Phys. Rev. Lett.* **105**, 090403 (2010).
[14] K. A. Milton, P. Parashar, N. Pourtolami and I. Brevik, *Phys. Rev. D* **85**, 025008 (2012).
[15] A. G. Kofman, G. Kurizki and B. Sherman, *J. Mod. Opt.* **41**, 353 (1994).
[16] M. Fujita, S. Takahashi, Y. Tanaka, T. Asano and S. Noda, *Science* **308**, 1296-1298 (2005).
[17] E. Shahmoon and G. Kurizki, *Phys. Rev. A* **87**, 033831 (2013).
[18] D. M. Pozar, *Microwave Engineering* (John Wiley and Sons, 2005).
[19] E. Shahmoon and G. Kurizki, arXiv:1302.2464 (2013).
[20] D. P. Craig and T. Thirunamachandran, *Molecular Quantum Electrodynamics* (Academic, London, 1984).
[21] C. Nguyen, *Analysis Methods for RF, Microwave, and Millimeter-Wave Planar Transmission Line Structures* (John Wiley and Sons 2000).
[22] L. DiCarlo, J. M. Chow, J. M. Gambetta, L. S. Bishop, B. R. Johnson, D. I. Schuster, J. Majer, A. Blais, L. Frunzio, S. M. Girvin and R. J. Schoelkopf, *Nature* **460**, 240-244 (2009).
[23] I.-C. Hoi, T. Palomaki, J. Lindkvist, G. Johansson, P. Delsing and C. M. Wilson, *Phys. Rev. Lett.* **108**, 263601 (2012).
[24] J. Koch, T. M. Yu, J. Gambetta, A. A. Houck, D. I. Schuster, J. Majer, A. Blais, M. H. Devoret, S. M. Girvin, and R. J. Schoelkopf, *Phys. Rev. A* **76**, 042319 (2007).
[25] M. Baur, A. Fedorov, L. Steffen, S. Filipp, M. P. da Silva and A. Wallraff, *Phys. Rev. Lett.* **108**, 040502 (2012).
[26] V. M. Stojanović, A. Fedorov, A. Wallraff and C. Bruder, *Phys. Rev. B* **85**, 054504 (2012).
[27] C. M. Wilson, G. Johansson, A. Pourkabirian, M. Simoen, J. R. Johansson, T. Duty, F. Nori and P. Delsing, *Nature* **479**, 376-379 (2011).
[28] A. André, D. DeMille, J. M. Doyle, M. D. Lukin, S. E. Maxwell, P. Rabl, R. J. Schoelkopf and P. A. Zoller, *Nature Phys.* **2**, 636-642 (2006).
[29] D. Petrosyan, G. Bensky, G. Kurizki, I. Mazets, J. Majer and J. Schmiedmayer, *Phys. Rev. A* **79**, 040304(R) (2009).
[30] D. Petrosyan and M. Fleischhauer, *Phys. Rev. Lett.* **100**, 170501 (2008).